Journal Homepage: http://ijcpe.uobaghdad.edu.iq
Iraqi Journal of Chemical and Petroleum Engineering
Vol. 26 No. 3 (September 2025) 183 – 191
EISSN: 2618-0707, PISSN: 1997-4884

Oxidation desulfurization of model oil using carbon composite derived from peach stone waste

Esraa Hashim Abood [a, *] , Haider A. Al-Jendeel [a], Sara Al-Salihi [b]

a Department of Chemical Engineering, College of Engineering, University of Baghdad, Aljadria, Baghdad, 10071, Iraq
b Biomedical, Biological and Chemical Engineering, University of Missouri, Columbia, MO, USA

Abstract

In this study, oxidative desulfurization of dibenzothiophene (DBT) with H_2O_2 as an oxidant was studied, whereas the catalyst used was zirconium oxide supported on Activated carbon (AC). Zirconium oxide (ZrO_2) was impregnated over prepared activated carbon (AC) and characterized by various techniques such as XRD, FTIR, BET, SEM, and EDX. This composite was used as a heterogeneous catalyst for oxidation desulfurization of simulated oil. The results of this study showed that ZrO_2/AC composite exhibited significant catalytic activity and stability, effectively lowering sulfur content under mild conditions. Factors such as reaction temperature (30, 40, 50, 60°C), time (5, 10, 15,20,30,60, 80 100 min), catalyst dose (0.3, 0.5, 0.7, 0.9 g) and initial concentration of dibenzothiophene (DBT) (20,40, 60, 80, 100, 200, 300 ppm) was used to achieved maximum efficiency. 10 ml of H_2O_2 /100 ml of simulated oil was used as an oxidizing agent. It was found that an increase in all the above variables led to an increase in desulfurization efficiency, except for an increase in initial DBT concentration, which led to a decrease in removal efficiency. The maximum removal efficiency of sulfur content was 92.22%, which was achieved at 60 $^{\circ C}$ and 0.9g of composite /100 ml of simulated oil at equilibrium time 100 min and 100ppm initial concentration of DBT. Finally, the reaction kinetics matched the pseudo-second order rate model, with an activation energy of 36.665 KJ/mol.

Keywords: Activated carbon; ZrO_2; simulated oil; oxidation desulfurization; Dibenzothiophene.

Received on 27/10/2024, Received in Revised Form on 17/01/2025, Accepted on 17/01/2025, Published on 30/09/2025

https://doi.org/10.31699/IJCPE.2025.3.15

1- Introduction

The petroleum industry has been greatly concerned with the development of transportation fuel that has a low sulfur level. This is because governments worldwide have imposed strict environmental [1]. The sulfur compounds found in fuel can be regarded as acidic and non-acidic. These compounds consist of sulfides, disulfides, mercaptans, thiophene and its related substances, such as benzothiophene, dibenzothiophenes, and 4,6-dimethyl dibenzothiophene. Any process that uses fuel, the organic sulfur compound type, will cause various pollutions, like sulfur dioxide (SOx), which will have a negative impact on the environment and human health. These pollutants are acid rain, global warming, air and water pollution, ecological instability, and harm to living things [2].

Desulfurization is crucial for managing sulfur levels in fuel and dealing with the problem of air pollution [3]. The catalytic hydrodesulfurization technique is mainly utilized for eliminating compounds containing sulfur from the petroleum product. Because it needs expensive conditions, including high temperature and pressure, as well as expensive catalysts, the hydrodesulfurization process is considered to be quite expensive [4].

Additionally, the HDS process can never exceed 100 ppm of sulfur content, even under extreme circumstances [5]. So that the researchers concentrate on non-HDS processes. Over the last decade, there has been a lot of research into oxidative desulfurization. ODS is a type of technology in which organic sulfur is oxidized by oxidants to strong polarity material. The reaction product can be extracted or absorbed to separate them. ODS operates at air pressure and temperatures below 100 ^{o}C, resulting in mild reaction conditions, no requirement for hydrogen, a pressure reactor, and specialized operational technology [6].

Transition metal oxide-impregnated activated carbon shows promise as an adsorbent for an extensive desulfurization method [7]. Likewise, the interaction between the active metal oxide and carbon support improves the physicochemical features of carbon-based catalysts [8]. Zirconia is one of the numerous inorganic oxides that has generated a lot of attention due to its use in a variety of applications, including adsorption, catalysis, and photo-degradation [9]. It is also considered a desirable material in a variety of industrial applications because of its high density, low cost, and outstanding textural properties like resistivity. Electrical, mechanical, thermal, and optical properties [10].

This study investigates the use of zirconia oxide (ZrO_2) supported on activated carbon, which was prepared from peach stones for the oxidative desulfurization of

*Corresponding Author: Email: esraa.abboud2207m@coeng.uobaghdad.edu.iq

simulated oil in the presence of H_2O_2 as an oxidant in a batch system.

2- Experimental section

2.1. Materials

The properties of chemical materials used in this work are shown in Table 1.

Table 1. Chemical materials used in research

Substance	chemical formula	molecular weight	purity %	supplier
n-Hexane	$CH_3(CH_2)_2CH_3$	86.18	95	CDH, India
Zirconia oxide	ZrO_2	123.218	99.9	Hongwu International Group Ltd
Polyvinyl Alcohol	[CH2CH(OH)]n	44.05	98	
Dibenzothiophene	C12H8S	184.26	97	India
Hydrogen peroxide	H_2O_2	34.01	35	ITW, Italy
Zinc chloride	$ZnCl_2$	136.28	98	India

2.2. Preparation of activated carbon

Activated carbon was prepared according to Gurung et al. [11], where peach stones were crushed and then sieved to get the raw material for the synthesized activated carbon. After that, the raw material reacted with $ZnCl_2$ to achieve chemical activation. Finally, that material was put in the oven for 3 hours at 500 ˚C in a tubular reactor to get activated carbon.

2.3. Preparation of ZrO_2/AC catalysts

Zirconia oxide loaded on activated carbon was prepared by the impregnation method, in which 22g of activated carbon was added to 1.54g of ZrO_2. First of all, AC was ground into powder shape, then it was dispersed in 100 ml of distilled water for the best dispersion. After that, 1.54g of ZrO_2 was dissolved in 20ml of distilled water, and then it was added to the dispersed AC in a dropwise. The obtained solution was mixed on a magnetic stirrer plate for 0.5 hours to get the best mixing. Then the solution was dried in an oven at 100 ˚C for 5 hours. Poly Vinyl Alcohol (PVA) was used as a bonding material between AC and ZrO_2. 6g of PVA was dissolved in 250ml of distilled water, then this solution was added to the sample of AC and ZrO_2. After that, this solution (AC, ZrO_2, and PVA) was dried in an oven at 80 ˚C for 24 hours.

2.4. Oxidation desulfurization process

100ml of n-hexane (used as simulated oil) was poured into a 250ml round-bottom flask with different initial concentrations of dibenzothiophene of 20,40, 60, 80, 100, 200, and 300 ppm. Several operating conditions were studied in a batch reactor, such as temperature (30, 40, 50, 60 ˚C), catalyst dosage (0.3, 0.5, 0.7, and 0.9) g/100ml of simulated oil, reaction time (5, 10, 15, 20, 30, 60, 80, 100 min), and 10 ml of H_2O_2. The batch reactor consists of a round-bottom flask with a water bath to control the temperature, a condenser, a magnetic stirrer, and a thermometer. The reactor was spun at a constant mixing speed of 650 rpm. When the solution reaches the desired temperature, H_2O_2 and the required amount of composite are added. After the reaction reached the desired time, the solution was filtered using filter paper, and the remaining solution was sent for sulfur analysis.

3- Results and discussion

3.1. Catalyst characterizations

3.1.1. X-ray diffraction

Fig. 1 shows the XRD pattern of ZrO_2/AC composite. It can be shown that the composite exhibits dual features, amorphous and crystalline structure, the peak position at 2Θ=20.19, 20.24, 41.36, 41.47 indicated the semi-crystalline nature of PVA [12]. The peaks at 24, 24.06, 28.51, 28.58, 31.78, 31.86, 34.63, 34.72, 50.51, 50.64, 61.37, 61.54 verify that ZrO_2 is present in the polymer matrix and AC [13]. Other peaks like 10.44, 10.47, 55.74, 55.90 belong to the monoclinic phase of ZrO_2 [14], and amorphous carbon is referred to by noisy background patterns.

3.1.2. EDX-SEM analyses

Fig. 2 shows SEM images of the prepared composite. As demonstrated, the composite had a rock-like form with uneven and diverse surface morphology. The sample shows the development of big, smooth particles; the biggest particle has a size of 920nm, while the smallest one has a size of 58.41nm. This result agrees with Yasin et al. [15]. While Table 2 shows EDX of the prepared composite, the elemental analysis reveals six atoms: carbon, oxygen, zirconium, zinc, copper, and chlorine. The Cu element is not involved in the composite synthesis, but it may come from the material that was used through the testing device. The carbon percent of the composite was 68.37% which indicates that peach stones were a good economical source for the production of activated carbon, and this agrees with Ahsaine et al. [16].

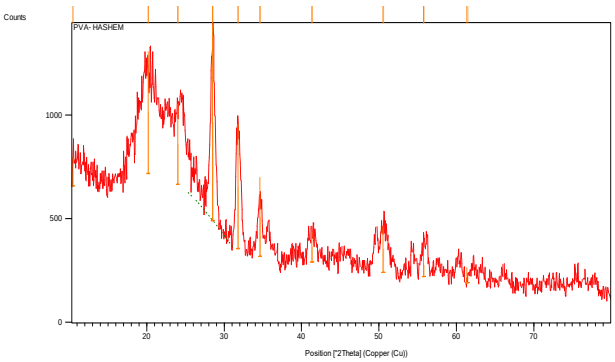

Fig. 1. XRD pattern of ZrO2/PVA/AC composite

3.1.3. N_2 adsorption-desorption isotherm

Textural properties were studied by N_2 adsorption-desorption isotherm. From Fig. 3, according to the

International Union of Pure and Applied Chemistry (IUPAC), ZrO_2/AC composite is classified as type IV, in which the structure is mesoporous, and this agrees with Thommes et al. [17]. The BET surface area is 730.95m^2g^{-1} with total pore volume 0.4003 cm^3 g^{-1} and average pore diameter of 2.1905nm.

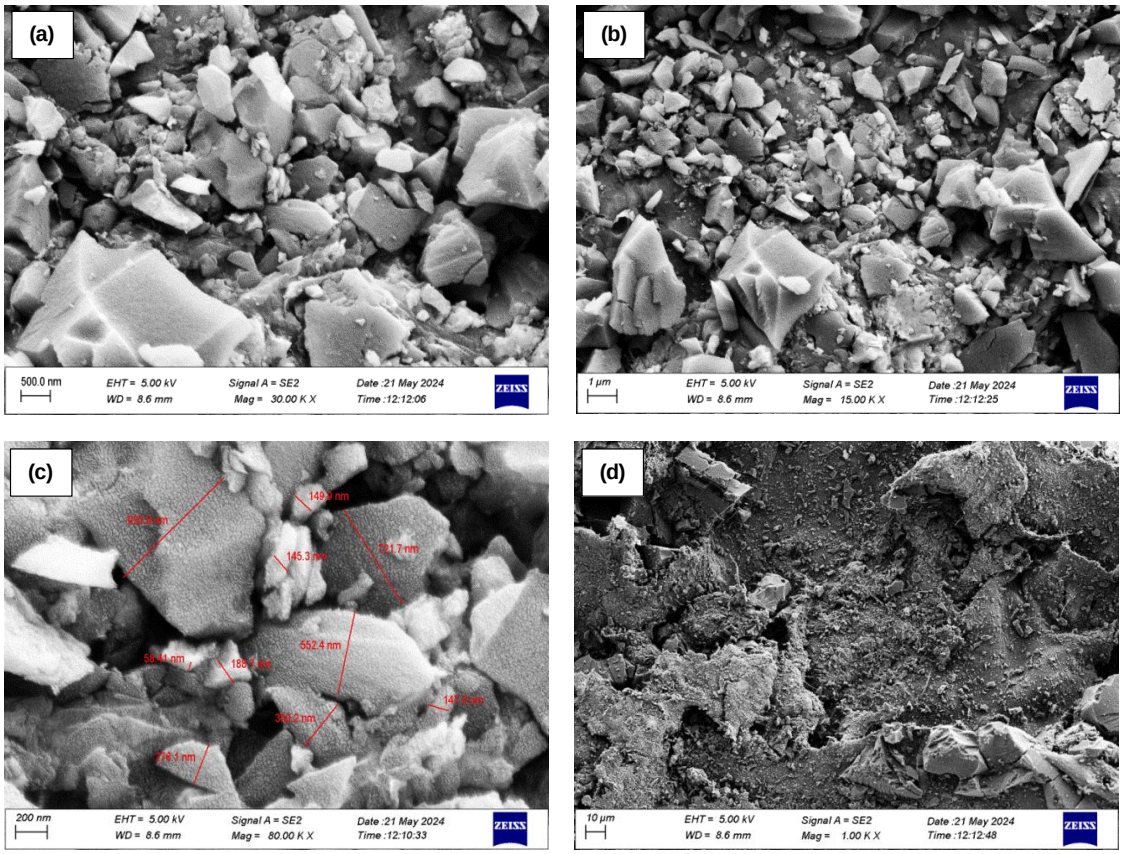

Fig. 2. SEM images of composite a) at 500nm, b) at 1µm, c) at 200nm d) at 10µm

Table 2. EDX analysis of the prepared composite

Element	Line type	Weight %	Weight % sigma	Atomic %
C	K Series	68.37	0.47	77.79
O	K Series	24.49	0.43	20.92
Zn	L Series	1.28	0.14	0.27
Zr	L Series	4.65	0.2	0.70
Cu	L Series	0.81	0.18	0.17
Cl	K Series	0.40	0.04	0.16
Total		100		100

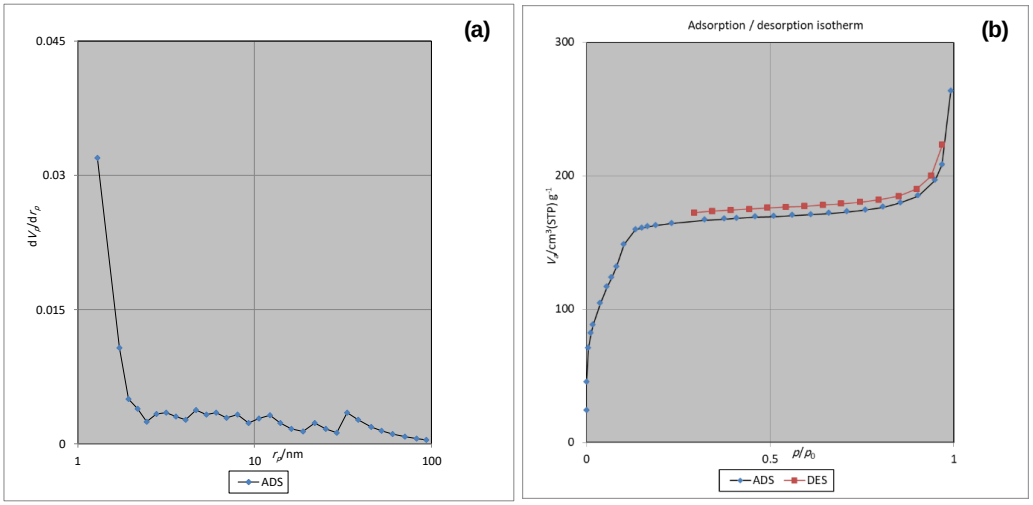

Fig. 3. a) pore size distribution of the composite. b) N_2 adsorption-desorption isotherm

3.1.4 AFM test

The AFM analysis provides a clear picture of the many data about the sample. The root mean square roughness (Sq) was determined to be 39.23nm from Table 3. Fig. 4 shows details about particle size distribution ranging between (5.676-238.3nm). The mean particle diameter was estimated to be 51.34nm, whereas the void volume was to be 43nm^3/nm^2.

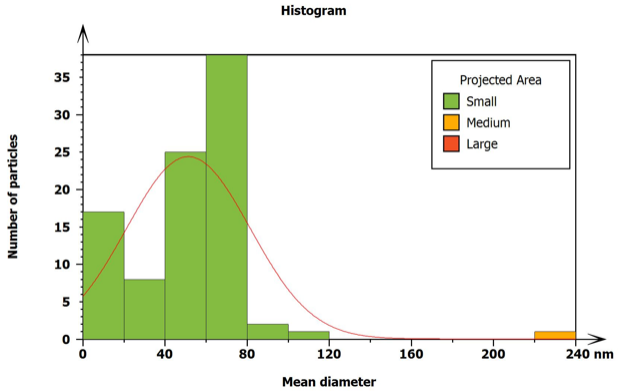

Fig. 4. Histogram of the prepared composite

Table 3. Height parameters of the composite

Height parameters	
Root mean square height (Sq)	39.23 nm
Skewness (Ssk)	-0.4189
Kurtosis (Sku)	1.725
Maximum peak height (Sp)	62.67nm
Maximum pit depth (Sv)	72.6nm
Maximum height (Sz)	135.3nm
Arithmetic mean height (Sa)	34.72nm

3.1.5. FTIR- spectrum of the composite

Fig. 5 shows that FTIR results often offer sufficient information regarding the functional groups present in the chemical structure of the materials [18].

The spectra illustrates 3381.21cm^{-1}, this peak was due to the stretching vibration of the O-H group. The peaks at 2951.09cm^{-1} and 2868.15cm^{-1} represented the C-H asymmetric and symmetric stretching. The band seen at 1687.71cm^{-1} can be assigned to C-OZr. The peaks at 1562.34 cm^{-1} and 1460.11cm^{-1} were attributed to Zr-OH [19]. The peak at 1400.32 cm^{-1} may refer to symmetric CO_2 stretch[20]. At around 1307.74 cm^{-1} and 887.26 cm^{-1}, the vinylidene C-H bend appears. The peak at 1155.36 cm^{-1} is associated with the C-O-C stretch. C-O stretch appears at 1093.64cm^{-1}. The band at 825.53cm^{-1} is assigned to the peroxides C-OO stretch. The band of 758.02cm^{-1} may be attributed to Zr-O [19]. The peak at 669.30 cm^{-1} is associated with the C-Br stretch. 599.86cm^{-1} represented the O-H out-of-plane bend [21]. From previous studies, the FTIR of PVA shows the major peaks associated with hydroxyl and acetate groups [22]. The peaks at 551.64 cm^{-1} and 520.78 cm^{-1} were attributed to Zr-O-Zr [23].

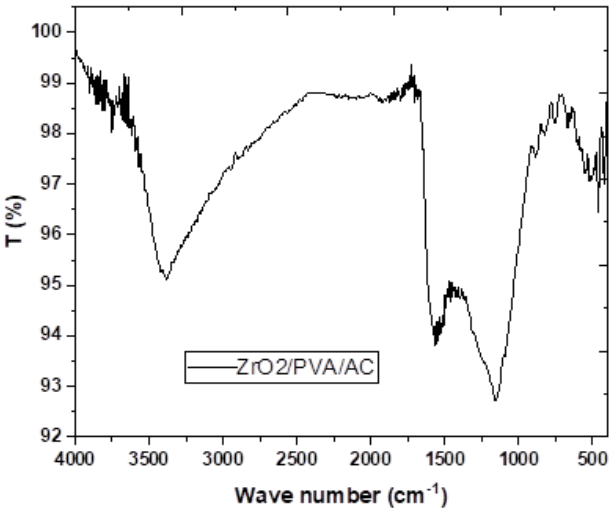

Fig. 5. FTIR of ZrO_2/AC composite

3.2. Operating condition test

3.2.1. Effect of temperature and time on desulfurization

The experiments were conducted at four distinct temperatures, specifically 30, 40, 50, and 60 ºC. The remaining experimental parameters, such as stirring speed 650 rpm, adsorbent dosage 0.5g, H_2O_2 (10ml), and beginning DBT concentration 105ppm, were held constant. The effect of time was experiment at the following intervals: 5, 10,15, 20, 30, 60, 80, and 100 min. Fig. 6 shows that at 60 °C, the removal efficiency was greatest, 90.59% at time 100 min, when the reaction reached equilibrium. It can be seen that the removal efficiency increased with an increase in both time and temperature. An increase in temperature will enhance the rate and kinetics of reaction, as well as higher temperatures are anticipated to enhance the diffusion of sulfur molecules, leading to an improved oxidation conversion. This result agrees with Xiong and Beshkoofeh [7, 24].

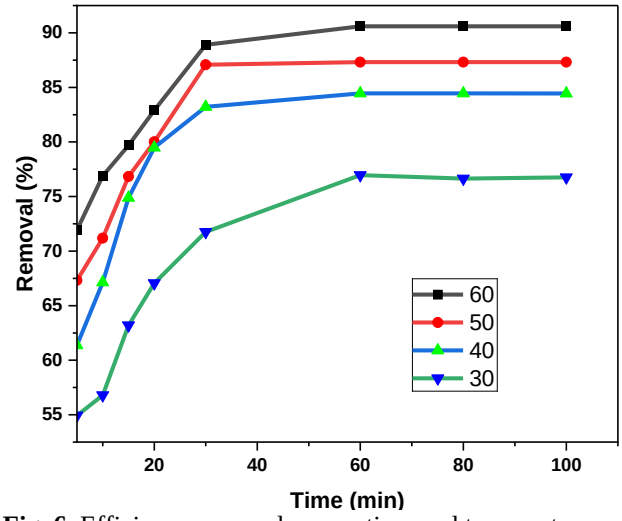

Fig. 6. Efficiency removal versus time and temperature

3.2.2. Effect of ZrO_2/AC dose on oxidative desulfurization

Fig. 7 illustrates the impact of the amount of catalyst 0.3, 0.5, 0.7, 0.9 measured in grams on the desulfurization of DBT. The experiments were conducted with a constant initial DBT concentration of 100 ppm, temperature of 60 °C, stirring speed of 650 rpm, 10 ml of H_2O_2, and an equilibrium time of 100 min. Because there were more adsorption sites and a bigger surface area available, the efficiency of removal percentage increased when the composite dose increased. This result confirms with Ahmed Zeki et al. [5].

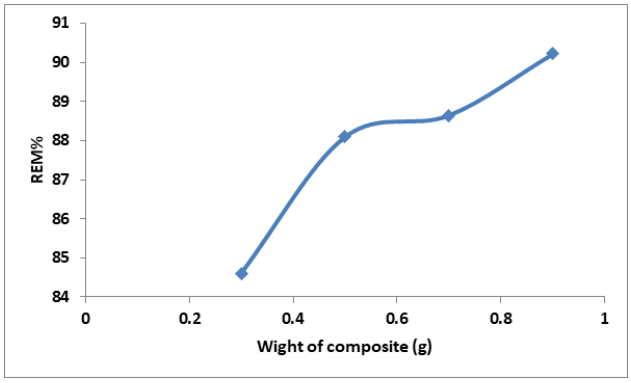

Fig. 7. Effect of composite dose on percent of removal

3.2.3. Effect of initial DBT concentration

Fig. 8 shows that the desulfurization efficiency varies with varying beginning amounts of sulfur content, which was examined using different concentrations of 20, 40, 60, 80, 100, 200, and 300 ppm. The desulfurization rate decreases as the initial sulfur content increases. In 100 min, the desulfurization efficiency of DBT reached 95.64% at starting sulfur content of 20 parts per million, as the initial sulfur concentration rose to 40, 60, 80, 100, 200ppm, subsequently to 300ppm, the desulfurization efficiency diminished from 94.19%, 93.76%, 91.19%, 90.59%, 86.338%, and then to 83.92% respectively. This is because the catalyst surface contains sulfones. This result was confirmed with Zhang et al. [25].

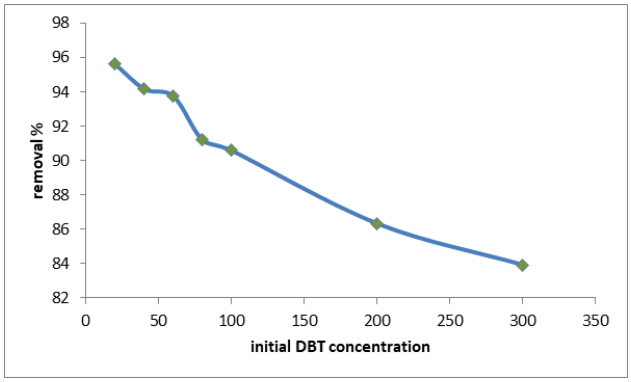

Fig. 8. Initial DBT concentration versus removal%

3.3. Catalytic kinetics

The kinetics of the ODS reaction were studied at various temperatures and times, with an optimal catalyst dose of 0.5g. total sulfur content was tested throughout time 5, 10, 15, 20, 30 min, and various temperatures 30, 40, 50, 60 °C. The ODS reactions with different DBT conversions followed the second-order reaction as shown in Fig. 9, Fig. 10, Fig. 11, and Fig. 12. However, the overall mechanism of DBT oxidation is summed up as follows:

$$C_{12}H_8S + 2H_2O_2 \rightarrow C_{12}H_6O_2S + 2H_2O + H_2 \quad (1)$$

The excess of hydroxyl radicals may be small in comparison to DBT concentrations, allowing for a simpler equation for future study:

$$\frac{d[C_{DBT}]}{dt} = K[C_{DBT}][OH] \quad (2)$$

$$\frac{1}{[C_{DBT}]t} = \frac{1}{[C_{DBT}]o} + Kt \quad (3)$$

Where $[C_{DBT}]_t$ and $[C_{DBT}]_o$ are the concentration of DBT at time t and at t=0

$$XA = \frac{[C_{DBT}]o - [C_{DBT}]t}{[C_{DBT}]o} \quad (4)$$

Substitution Eq. 4 in Eq. 3 to get:

$$\frac{XA}{(1-XA)} = K[C_{DBT}]o \quad (5)$$

Where XA represents the conversion of DBT.

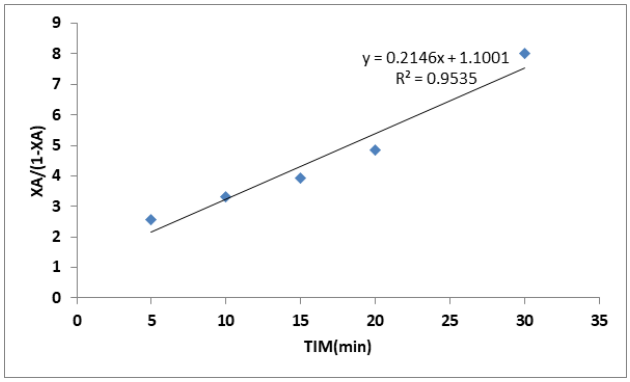

Fig. 9. Pseudo-second order reaction rate equation at a temperature of 60 °C

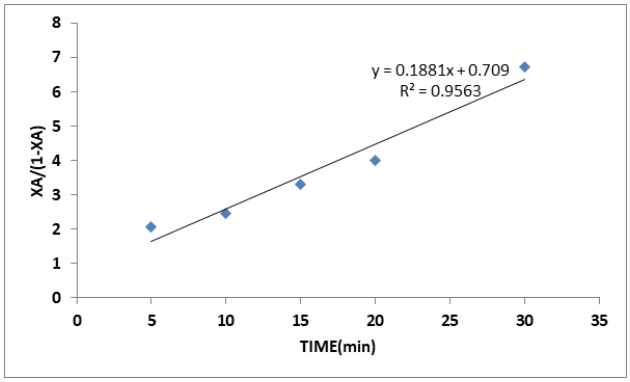

Fig. 10. Pseudo-second order reaction rate equation at a temperature of 50 °C

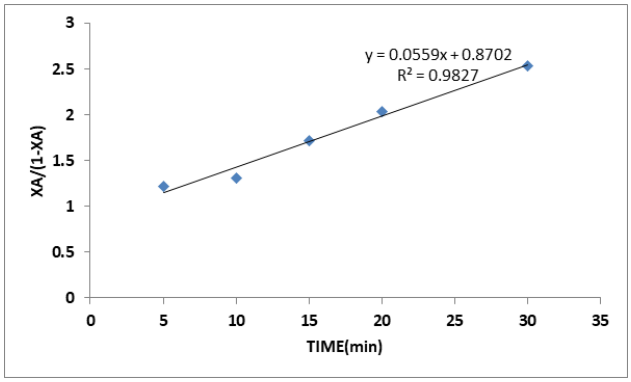

Fig. 11. Pseudo-second order reaction rate equation at a temperature of 30 °C

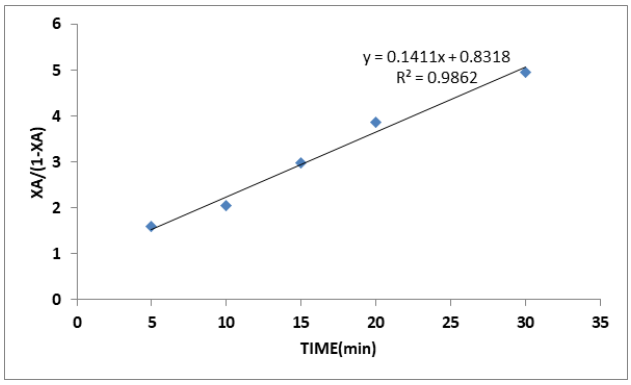

Fig. 12. Pseudo-second order reaction rate equation at a temperature of 40 °C

The R^2-value correlation coefficients for curve fitting and rate constants are shown in Table 4. The reaction rate constant increases with increasing temperature of the reaction because it's highly temperature-dependent.

Table 4. The reaction rate constant is calculated using a power law model at different temperatures

Temperature (K)	Rate constant	R^2
303	98.07	0.9827
313	247.544	0.9862
323	330	0.9563
333	376.491	0.9535

The activation energy of sulfur removal reactions was estimated using the Arrhenius equation, which is as follows:

$$K = Aexp(\frac{-E_a}{RT}) \quad (6)$$

Where A is a pre-experimental factor, and Ea is the activation energy (KJ/mol); R, the gas constant, which equals 8.314 J/mol.K. K was the pseudo-second order constant. Fig. 13 includes a plot of ln(K) vs 1/T. The Ea of the DBT oxidation process was determined as 36.665 KJ/mol based on the curve slope.

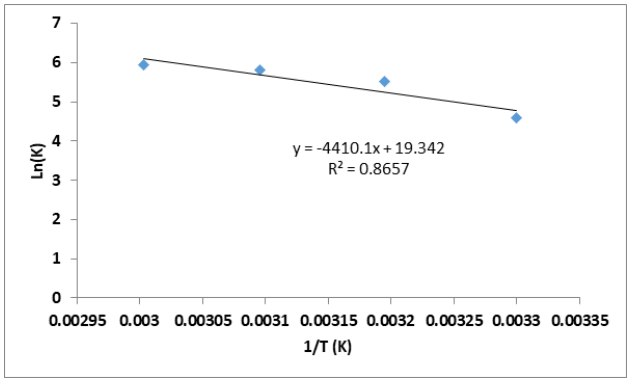

Fig. 13. the plot of ln(K) vs. 1/T

4- Conclusion

ZrO_2/AC composite was produced by using the impregnation method and tested in the oxidation desulfurization of simulated oil. The effect of different parameters, such as time, temperature, composite dose, and initial DBT concentration, on DBT removal efficiency was investigated in this study. It was found that the removal efficiency increases with an increase in time, temperature, and composite dose, while it decreases with an increase in initial DBT concentration. The optimum DBT conversion was 92.22%, which was achieved at 60 °C and 0.9g of composite /100 ml of simulated oil at equilibrium time 100 min and 100ppm initial concentration of DBT. Finally, the reaction kinetics matched the pseudo-second order rate model, with an activation energy of 36.665 KJ/mol.

Conflict of Interest

The authors declare that there is no conflict of interest.

References

[1] T. A. Jalal and L. F. Hasan, "oxidative desulfurization of gasoil using improving selectivity for active carbon of rice husk", *Diyala Journal For Pure Science*, vol:8, no. 3, 2012.

[2] A.T. Nawaf and B. A. Abdulmajeed, "Design of oscillatory helical baffled reactor and dual functional mesoporous catalyst for oxidative desulfurization of real diesel fuel", *Chemical Engineering Research and Design*, vol. 209, pp.193-209, 2024. http://doi.org/10.1016/j.cherd.2024.07.032

[3] N. M. Abdullah, H. Q. Hussien, and R. R. Jalil, "Heavy Naphtha Desulfurization by ozone generated via the DBD plasma reactor" *Iraqi Journal of Chemical and Petroleum Engineering* , vol.25 no. 2 pp.131-137, 2024. https://doi.org/10.31699/IJCPE.2024.2.12

[4] S. H. Ammar and S. A. Jaafar "Adsorption kinetic and isotherms studies of thiophene removal from model fuel on activated carbon supported copper oxide". *Iraqi Journal of Chemical and Petroleum Engineering*, vol.18, no.2, pp. 83-93, 2017. https://doi.org/10.31699/IJCPE.2017.2.7

[5] N. S. Ahmed Zeki, S. M. Ali, and S. R. Al-Karkhi "Investigation desulfurization method using air and zinc oxide/ activated carbon composite". *Iraqi Journal of Chemical and Petroleum Engineering*, vol.18, no.1, pp. 37-46, 2017. https://doi.org/10.31699/IJCPE.2017.1.3

[6] G. Zhang, F. Yu, and R. Wang, "Research advances in oxidative desulfurization technologies for the production of low sulfur fuel oils", *Petroleum And Coal*, 51(3) 196-207, 2009.

[7] L. Xiong, X. M. Yan, and P. Mei,. "Synthesis and characterization of a ZrO2/AC composite as a novel adsorbent for dibenzothiophene". *Adsorption Science and Technology*, vol. 28 no. 4, pp.314-350, 2010. https://doi.org/10.1260/0263-6174.28.4.341

[8] Y. Li, X. Tang, S. Niu, Y. Wang, K. Han, and C. Lu, . "synthesis of the zirconium dioxide activated carbon based heterogeneous acid catalyst to catalyze esterification for biodiesel production with molecular simulation", *Biomass Conversion And Biorefinery*, vol.13(17), 2023. https://doi.org/10.1007/s13399-021-02105-5

[9] Z. Hassan, D. O. Cho, I. H. Nam, C. M. Chon, and H. Song," Preparation of calcined zirconia-carbon composite from metal organic frameworks and its application to adsorption of crystal violet and salicylic acid", *Materials*, vol.9, 261, 2016. https://doi.org/10.3390/ma9040261

[10] A. Elmouwahidi, E. B. Garcia, A. F.P Cadenas., F. J. M. Hodar. , J. C. Quiben, and F. C. Marin. "Electrochemical performances of supercapacitors from carbon-ZrO2 composite", *Electrochimica Acta*, vol. 259, pp.803-814, 2018. https://doi.org/10.1016/j.electacta.2017.11.041

[11] V. Gurung, B. Pokharel et al., "Characterization of activated carbon prepared from peach seed stone by chemical activation with zinc chloride ($ZnCl_2$)", *Proceeding of IOE Graduate Conference*, vol.7, pp.59-64, 2019.

[12] R. Kandulna, R. B. Choudhary. "Concentration-dependent behaviors of ZnO-reinforced PVA-ZnO nanocomposites as electron transport materials for OLED application", *Polymer Bulletin*, vol. 75, 2018. https://doi.org/10.1007/s00289-017-2186-9

[13] K. Krishnamoorthy, S. Natarajan, S. Kim, and J. Kadarkaraithangam, "Enhancement in thermal and tensile properties of ZrO2/poly (vinyl alcohol) nanocomposite film", *Materials Express*, vol.1, no. 4, 2011. https://doi.org/10.1166/mex.2011.1036

[14] S. Ding, J. Zhao, and Q. Yu. "Effect of zirconia polymorph on vapor phase ketonization of propionic acid". *Catalysts*, vol.9, p.768, 2019. https://doi.org/10.3390/catal9090768

[15] A. S. Yasin, M. Obaid, I. M. A. Mohamed, A. Yousef, and N. A. M. Barakat. "ZrO_2 nanofibers/AC composite as a novel and effective electrode material for the enhancement of capacitive deionization performance". *RSC Adv*ances, vol.7, 4616, 2017. https://doi.org/10.1039/c6ra26039j

[16] H. A. Ahsaine, Z. Anfar, M. Zbair, M. Ezahri, and N. El Alem. "Adsorption removal of methylene blue and crystal violet onto micro-mesoporous Zr3O/Activated carbon composite: a joint experimental and statistical modeling considerations" *Journal of Chemistry*. 2018. https://doi.org/10.1155/2018/6982014

[17] M. Thommes, K. Kaneko, A. V. Neimark, J. P. Olivier, F. R. Reinoso, J. Rouquerol, and K. S. W. Sing, . "Physisorption of gases, with special reference to the evaluation of surface area and pore size distribution (IUPAC technical report). *Pure Appllied Chem*istry, vol. 87, no. 9-10, pp.1051-1069, 2015. https://doi.org/10.1515/pac-2014-1117

[18] P. Praveen, G. Viruthagiri, S. Mugundan, and N. Shanmugam, "structural and optical and morphological analyses of pristine titanium di-oxide nanoparticals-synthesized via sol-gel route", *Spectrochimica Acta Part A: Molecular And Biomolecular Spectroscopy*, vol.117, pp. 622-629, 2014. https://dx.doi.org/10.1016/j.saa.2013.09.037

[19] P. N. Chuc et al. "Highly efficient adsorption of arsenite from aqueous by zirconia modified activated carbon". *Environmental Engineering Research* vol. 29(2), 2024. https://doi.org/10.4491/eer.2023.076

[20] B. C. Smith. "The carbonyl group, part V: carboxylates- coming clean". *Spectroscopy*, vol. 33 pp. 20-23, 2018.

[21] A. B. D. Nandiyanto, R. Oktiani, and R. Ragadhita. "How to read and interpret FTIR spectroscope of organic material". *Indonesian Journal of Science & Technology*, vol.4(1) pp.97-118, 2019.

[22] H. S. Mansur, C. M. Sadahira, A. N. Souza, A. A. P. Mansur. "FTIR spectroscopy characterization of polyvinyl alcohol hydrogel with different hydrolysis degrees and chemically crosslinked with glutaraldehyde". *Material Science And Engineering*, vol.28, pp. 539-548, 2008. https://doi.org/10.1016/j.msec.2007.10.088

[23] N. F. M. Suhaimi, S. A. Kamil, and M. K. Abd Rahman, "morphological, structural, and photoluminescence properties of Er^{+3} doped SiO2-ZrO2/PVA nanofiber". *Journal of Engineering and Science and Technology*, vol.18, pp. 437-452, 2023.

[24] S. Beshkoofeh, B. G. Choobar, and Z. Shahidian, "Optimization of the oxidative desulfurization process of light cycle oil with NiMo/y Al_2O_3 catalyst". *Physical Chemistry Research*, vol.10, no.1, pp. 57-67, 2022. https://doi.org/10.22036/PCR.2021.285150.1917

[25] X. Zhang, Y. Zhu, Q. Han, X. MA, P. Chen Z., Zhao, and Q. Wang, " Pd $(CH_3COOH)_2$ and MIL-101 (Cr) composites: A novel in-situ oxidation catalyst for the removal of BT from fuel oil under natural condition", *IOS Press Ebooks*, vol.22, pp.331-339, 2022. https://doi.org/10.3233/ATDE220245

[26] A. E. S. Choi, S. Roces, N. Dugos, and M.W. Wan, "Mixing-assisted oxidative desulfurization of model sulfur compounds using polyoxometalate/H2O catalytic system", *Sustainable Environment Research*, vol. 26, pp.184-190, 2016. https://doi.org/10.1016/j.serj.2015.11.005

[27] P. Huang, G. Luo, L. Kang, M. Zhu, and B. Dai, "Preparation, characterization and catalytic performance of HPW/aEVM catalyst on oxidative desulfurization", *RSC Advances*, vol. 7, pp. 4681-4687, 2017. https://doi.org/10.1039/C6RA26587A

[28] H. H. Alwan, A. A. Ali, and H. F. Makki, "Optimization of oxidative desulfurization reaction with Fe_2O_3 catalyst supported on graphene using box-behnken experimental method", *Bulletin of Chemical Reaction Engineering and Catalysis*, vol. 15, pp.175-185, 2020. https://doi.org/10.9767/bcrec.15.1.6670.175-185

ازالة الكبريت من الزيت المحاكي عن طريق الأكسدة باستخدام مركب الكربون المشتق من نفايات بذور الخوخ

اسراء هاشم عبود [١، *]، حيدر عبدالكريم الجنديل [١]، سارة الصالحي [٢]

١ قسم الهندسة الكيمياوية ، كلية الهندسة، جامعة بغداد، بغداد، العراق
٢ الهندسة الطبية الحيوية والبيولوجية والكيميائية، جامعة ميسوري، كولومبيا، ميسوري، الولايات المتحدة الأمريكية

الخلاصة

في هذه الدراسة، تمت دراسة ازالة الكبريت المؤكسد من ثنائي بنزوثيوفين (DBT) باستخدام بيروكسيد الهيدروجين كعامل مؤكسد، و اوكسيد الزركونيوم المحمل على الكاربون المنشط كعامل مساعد. تم تشريب اوكسيد الزركونيوم فوق الكاربون المنشط المحضر و توصيفه بتقنيات مختلفة مثل XRD, FTIR, BET, SEM, EDX. تم استخدام هذا المركب كمحفز غير متجانس لإزالة الكبريت بعملية الاكسدة من الزيت المحاكي. اظهرت نتائج هذه الدراسة ان مركب ZrO2 /AC اظهر نشاطاً تحفيزياً واستقراراً كبيراً، مما ادى بشكل فعال الى خفض محتوى الكبريت في ضل ظروف معتدلة. تم دراسة عدة عوامل مثل درجة حرارة التفاعل (٣٠, ٤٠, ٥٠, ٦٠ درجة مئوية)، والوقت (٥, ١٠, ١٥, ٢٠, ٣٠, ٦٠, ٨٠, ١٠٠ دقيقة)، وكمية العامل المحفز (٠,٣, ٠,٥, ٠,٧, ٠,٩ غرام) والتركيز الابتدائي للداي بنزوثيوفين (٢٠, ٤٠, ٦٠, ٨٠, ١٠٠, ٢٠٠, ٣٠٠ جزء من المليون) لتحقيق اقصى قدر من الكفاءة. تم استخدام ١٠ مل من بيروكسيد الهيدروجين/ ١٠٠ مل من الزيت المحاكي كعامل مؤكسد. وجد ان الزيادة في كل المتغيرات المذكورة اعلاه ادت الى زيادة في كفاءة ازالة الكبريت باستثناء الزيادة في التركيز الابتدائي للداي بنزوثيوفين. بلغت اقصى كفاءة لإزالة محتوى الكبريت ٩٢,٢٢% والتي تم تحقيقها عند درجة حرارة ٦٠ درجة مئوية و ٠,٩ غرام من العامل المساعد عند زمن ١٠٠ دقيقة وتركيز ابتدائي ١٠٠ جزء من المليون من داي بنزوثيوفين. تطابقت حركة التفاعل مع نموذج معدل من الدرجة الثانية، حيث بلغت طاقة التنشيط ٣٦,٦٦٥ كيلو جول/مول.

الكلمات الدالة: الكربون المنشط، ZrO2، زيت محاكى، أكسدة الكبريت، ثنائي بنزوثيوفين.